Computational and Structural Biotechnology Journal 19 (2021) 5578–5588

COMPUTATIONAL AND STRUCTURAL BIOTECHNOLOGY JOURNAL

journal homepage: www.elsevier.com/locate/csbj

Dual roles of SIRT1 in the BAX switch through the P53 module: A mathematical modeling study

Nan Liu [a], Hongli Yang [a,*], Liangui Yang [a]

[a] School of Mathematical Sciences, Inner Mongolia University, Hohhot 010021, China

ARTICLE INFO

Article history:
Received 9 August 2021
Received in revised form 25 September 2021
Accepted 28 September 2021
Available online 02 October 2021

Keywords:
SIRT1
P53-MDM2
BAX switch
Apoptosis
Bifurcation

ABSTRACT

SIRT1 is a multifunctional deacetylase that participates in a variety of cellular physiological processes to cope with stress. The anticancer protein P53 is an important target of SIRT1. It has been found that SIRT1 is involved in apoptosis by regulating the activity and intracellular location of P53. Moreover, P53-dependent apoptosis is inseparable from the **BCL-2** protein family. Among the members of this family, BAX's switching dynamics may play a key role in apoptosis. Therefore, a challenging question arises: what effect does SIRT1 have on the BAX switch? To answer this question, we built a small-scale protein network model. Through computer simulation, the properties of SIRT1 that on the one hand promote and on the other inhibit apoptosis are revealed. We found that the opening time of the BAX switch will be delayed in the case of either SIRT1 excess or deficiency. Similarly, the stimulus threshold required for apoptosis will also increase in the above two scenarios. Thereby, we proposed that SIRT1 has an optimal content at which the probability of apoptosis is greatest. In addition, P53 oscillation requires the concentration of SIRT1 to be higher than the optimal value. This work may be helpful both experimentally and clinically.

1. Introduction

The bistable switch is a mathematically well-studied nonlinear dynamic behavior that transforms a continuous input signal into two discrete outputs, leading to a large gap between outcomes [1]. Cells apply the bistable switch to make a reliable decision, avoiding ambiguous situations. An experimental-data-based mathematical modeling case is the E2F switch [2]. This switch is responsible for cell proliferation. Moreover, many other gene network motifs possess a positive feedback loop (PFL) and have the potential to generate a bistable switch from a theoretical point of view [3–5]. In this work, we focused on the BAX switch, a marker of apoptosis, to address the question of how Sirtuin1 protein (SIRT1) regulates the cell fate induction.

BAX is a member of the B-cell lymphoma-2 (**BCL-2**) family that targets the mitochondrial outer membrane (MOM) to carry out its function [6]. By controlling mitochondrial outer membrane permeabilization (MOMP), BAX can release proapoptotic factors such as cytochrome c from mitochondria to the cytosol [7]. Therefore, BAX (or more generally, BAX-like proteins, e.g., BAK and BOK [8]) plays a key role in the intrinsic programmed cell death pathway. In resting cells,BAX is mainly located in the cytosol due to loose attachment to the MOM [6]. The pro-survival class of **BCL-2** family members (for a simple description, we useBCL-2 hereafter) is the dominant inhibitor of BAX [9]. It is suggested that the BH3-only proteins (PUMA, BAD, etc.), which are other pro-apoptotic members of the **BCL-2** family, promote the BAX activation (i.e., translocation to MOM) [10]. As considered in many mathematical modeling studies [4,11–13], BCL-2 blocks the BAX activation by binding the BH3-only proteins. In turn, active BAX also reduces the inhibitory function of BCL-2 by binding, forming a PFL. This is a design principle for the BAX switch [12]. One of the characteristics of cancer cells is resistance to apoptosis; thus, there is no doubt that the BAX switch is an essential target for tumor treatment [14]. Typically, in response to DNA damage stimuli, the P53 module acts as a sensor to transmit proapoptotic signals to the downstream effector, i.e., apoptotic module [12,13,15–17]. Although there are other upstream and downstream proteins on the BAX switch [18], this is beyond the scope of our research and will not be discussed.

P53 is a powerful transcription factor. Its target genes are involved in various cellular events, including DNA damage repair, cell cycle arrest, and apoptosis [19]. As the most famous tumor suppressor, it has been reported that more than 50% of human cancers contein P53 mutations [20]. In addition, many experiments have observed P53 oscillation in vivo and in vitro and across spe-

* Corresponding author.
E-mail address: imuyhl@imu.edu.cn (H. Yang).

https://doi.org/10.1016/j.csbj.2021.09.033

cies [21–23]. More importantly, cell fate is regulated by P53 dynamics [24]. These facts have driven a number of theoretical studies to identify the potential dynamics of P53 controlled by its key regulator using the bifurcation method [25–30]. The mainstream point of view is that P53 oscillation requires a P53-MDM2 negative feedback loop (NFL) gene network structure. That is, P53 transactivates the Mdm2 gene, but MDM2 reduces P53 levels through the ubiquitin–proteasome pathway [31]. However, unless a time delay is added, a single NFL is not sufficient to generate oscillations [32]. In this regard, the time delay can be derived from the time spent on transcription, translation and transmembrane localization of MDM2 [27]. Alternatively, the time delay can be hidden in ordinary differential equation (ODE) models by dividing the nucleocytoplasmic region or connecting a PFL [33–35]. Clearly, great progress has been made in understanding the kinetics of the pure P53 module. However, in our opinion, building the crosstalk models between the P53 module and the apoptotic module to probe the sophisticated cell fate decision mechanism mediated by the temporal P53 dynamics maximizes the advantages of computing on the one hand and may be more useful for clinical applications on the other.

There are many ways in which P53 affects **BCL-2** family proteins. The promoters of BAX and its activator PUMA are both direct targets of P53 [36,37]. In addition, P53 can induce the expression of a class of micro RNA, miR-34, to repress BCL-2 levels [38,39]. These effects of P53 depend on transcription and contribute to the MOMP, namely, the transcription-dependent apoptosis of P53. Correspondingly, there is the transcription-independent apoptosis of P53 [40]. P53 in cytoplasm forms a complex with BCL-2 as part of a novel mechanism to induce the MOMP [41]. Subsequently, theoretical studies have considered cooperation between P53 transcription-dependent and transcription-independent apoptotic pathways and pointed out that both nuclear and cytoplasmic P53 activities are important for reliable cell fate decisions [42,43]. However, how SIRT1, a negative regulator of P53, mediates P53 dynamics and further apoptosis is still not fully understood.

As reviewed by Yi and Luo [44], SIRT1 was initially considered a tumor promoter. Later, growing evidence has proven that SIRT1 plays a dual role in tumorigenesis. On the one hand, SIRT1 reduces the transcription ability of P53 through deacetylation [45], which is harmful to transcription-dependent apoptosis. On the other hand, SIRT1-catalyzed deacetylated P53 is more easily stored in the cytoplasm, enhancing transcription-independent apoptosis [46]. Therefore, it is not surprising that SIRT1 is elevated in leukemia and prostate cancer [47,48], but decreased in breast cancer and liver cancer [49]. Nevertheless, theoretical insights still need to be improved.

Motivated by the above considerations, we develop an ODE model of the connection between the P53 module and the BAX switch. Our innovation is embodied in theoretically confirming the dual role of SIRT1 in apoptosis. This ODE model is supported by some known biological facts. Consequently, we predict that there is an optimal concentration of SIRT1 at which the cells are most sensitive to genotoxic stress; the BAX switch is difficult to turn on with the low SIRT1 levels; when the SIRT1 level is high, cells may undergo P53-oscillation-mediated cell cycle arrest instead of apoptosis initiation if the DNA damage level is not high enough. These results may provide design ideas for molecular biology experiments and specific anticancer drugs.

2. Materials and methods

2.1. Model overview

There are many existing models to describe the switching behavior underlying the interactions of the**BCL-2** family members [4,11–13]. We choose the model in [12] to expand. The authors made use of the PFL of double negative regulation between BAX and BCL-2 to produce a bistable switch [12], as shown in Fig. 1. Initially, DNA damage promotes P53, which is reflected in the enhancement of stability and DNA binding ability of P53 [50]. Then, the increased P53 molecule not only induces the synthesis of pro-apoptotic proteins and/or noncoding RNA but also diffuses into the cytoplasm, thereby turning on the apoptotic switch [42]. We call the former the indirect pathway and the latter the direct pathway in Fig. 1. Obviously, SIRT1 promotes the direct pathway but inhibits the indirect pathway [44]. Moreover, it is assumed that if P53 binds to BCL-2, it cannot cross the nuclear membrane to regain transcription factor activity. Thus, the direct pathway fundamentally suppresses the indirect pathway in our model.

2.2. Model details

The complete protein network model we constructed is shown in Fig. 2. For simplicity, we only consider one branch of the P53-mediated indirect apoptotic pathway, that is, P53 transactivates the BH3-only proteins (labeled as BH3 in Fig. 2) [37]. Furthermore, the P53 module contains only two types of proteins, i.e., P53 and MDM2. Taken together, we want to use fewer network nodes and more streamlined node relationships to explore the issues we care about. Here, P53 is divided into four subcategories: active P53 in the nucleus (P53na) and cytoplasm (P53ca), and inactive P53 in the nucleus (P53n) and cytoplasm (P53c). It is assumed that unmodified P53 (P53c) and (P53n) can enter and exit the nucleus freely, unlike activated (phosphorylated and/or acetylated) P53 that is confined to the nucleus [32]. Therefore, P53ca can enter the nucleus, but P53na cannot enter the cytoplasm in our model. Similarly, MDM2 is divided into three subcategories: phosphorylated MDM2 in the nucleus (MDM2np) and cytoplasm (MDM2cp) and unmodified MDM2 in the cytoplasm (MDM2c). The reason why there is no unmodified MDM2 in the nucleus is that the prerequisite for MDM2 to shuttle through the nuclear membrane is for it to be phosphorylated [51]. In addition, we assume that the intracellular sublocalization of SIRT1 is not restricted, while the **BCL-2** family only exists in the cytoplasm. We use [P] to denote the concentration of protein P. The protein subclasses appearing in the ODEs are listed in Table 1. The ODEs and their meanings are shown below.

For SIRT1, its synthesis site is the cytoplasm, which corresponds to the term k_{ssirt} in Eq. 1. The second and last terms on the right side of Eq. 1 represent the degradation and transmembrane diffusion of SIRT1, respectively. Of note, the last terms of Eqs. 1 and 2 have the same meaning. When the protein in the cytoplasm flows into the nucleus, the increased concentration in the nucleus is greater than the decreased concentration in the cytoplasm. Therefore, the ratio of cytoplasm to nucleus V_{r} needs to be multiplied by the diffusion term of Eq. 2 [32,52].

$$\frac{\mathrm{d}[\mathrm{SIRT1c}]}{\mathrm{d}t} = k_{\mathrm{ssirt}} - k_{\mathrm{dsirt}}[\mathrm{SIRT1c}] - k_{\mathrm{i}}([\mathrm{SIRT1c}] - [\mathrm{SIRT1n}]), \tag{1}$$

$$\frac{\mathrm{d}[\mathrm{SIRT1n}]}{\mathrm{d}t} = -k_{\mathrm{dsirt}}[\mathrm{SIRT1n}] + V_{\mathrm{r}}k_{\mathrm{i}}([\mathrm{SIRT1c}] - [\mathrm{SIRT1n}]). \tag{2}$$

The equation forms of P53 are slightly complicated due to the enzymatic reactions, which follow Michaelis–Menten kinetics [15,16]. The first term on the right side of Eq. 3 is the basal activation of P53n, the second term is P53n activation caused by DNA damage (represented by [Dam]), the third term is P53na inactivation catalyzed by SIRT1, and the fourth term is P53na degradation induced by MDM2. Compared with inactive P53, active P53 is difficult to degrade [53]. Thus, the degradation rate of inactive P53 is relatively large, and there is a basal degradation term in the equa-

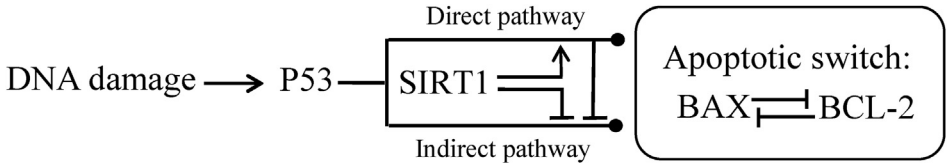

Fig. 1. Concise schematic diagram of the model. P53 is similar to a sensor that transmits DNA damage signals to the apoptotic switch through direct (transcription-independent) and indirect (transcription-dependent) pathways. The switch dynamics behavior depends on the mutual inhibition of BAX andBCL-2. The direct pathway weakens the indirect pathway, and SIRT1 increases the signal flow distribution of the direct pathway. The promotion is represented by arrowheaded lines, the inhibition is denoted by bar headed lines, and the transmission of the apoptotic signals is marked with circle-headed lines.

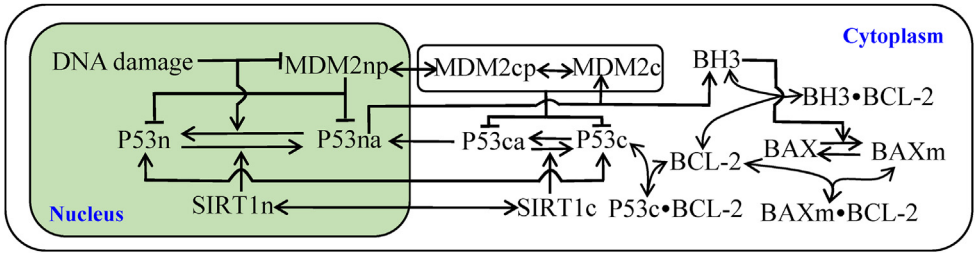

Fig. 2. Schematic diagram of the protein network. Pn and Pc represent protein P in the nucleus and cytoplasm, respectively. a, p, and m at the end of P53, MDM2, and BAX represent activation, phosphorylation, and insertion into the outer mitochondrial membrane, respectively. A•B represents the complex formed by proteins A and B. The promotion and state transition are represented by arrowheaded lines, and the inhibition is denoted by bar-headed lines.

Table 1
Protein subclasses in the equations.

Protein subclass	Description
P53na	Active P53 in the nucleus.
P53n	Inactive P53 in the nucleus.
P53ca	Active P53 in the cytoplasm.
P53c	Inactive P53 in the cytoplasm.
MDM2c	Unmodified MDM2 in the cytoplasm.
MDM2cp	Phosphorylated MDM2 (at Ser-166 and/or Ser-168) in the cytoplasm.
MDM2np	Phosphorylated MDM2 (at Ser-166 and/or Ser-168) in the nucleus.
SIRT1c	SIRT1 in the cytoplasm.
SIRT1n	SIRT1 in the nucleus.
BCL – 2	BCL-2 monomer.
BH3	BH3 monomer.
BAX	BAX monomer.
P53c • BCL – 2	Complex of P53 and BCL-2.
BH3 • BCL – 2	Complex of BH3 and BCL-2.
BAXm	BAX monomer inserted on the outer mitochondrial membrane.
BAXm • BCL – 2	Complex of BAXm and BCL-2.
BCL – 2total	The total amount of BCL-2.
BH3total	The total amount of BH3.
BAXtotal	The total amount of BAX.

tions of inactive P53, such as the penultimate term of Eq. 4. In addition, the last two terms of Eq. 5 represent the association and dissociation of P53c and BCL-2, following the law of mass action.

$$\frac{d[P53na]}{dt} = k_{acp530}[P53n] + k_{acp531}\frac{[Dam]}{[Dam]+j_{dam}}[P53n] - k_{dep53}\frac{[SIRT1n]}{[SIRT1n]+j_{sirt1}}[P53na] - k_{dp53s}[MDM2np]\frac{[P53na]}{[P53na]+j_{1p53}} + V_r k_i[P53ca], \tag{3}$$

$$\frac{d[P53n]}{dt} = -k_{acp530}[P53n] - k_{acp531}\frac{[Dam]}{[Dam]+j_{dam}}[P53n] + k_{dep53}\frac{[SIRT1n]}{[SIRT1n]+j_{sirt1}}[P53na] - k_{dp53}[MDM2np]\frac{[P53n]}{[P53n]+j_{1p53}} - k_{dp530}[P53n] + V_r k_i([P53c] - [P53n]), \tag{4}$$

$$\frac{d[P53c]}{dt} = k_{sp53} - k_{acp530}[P53c] + k_{dep53}\frac{[SIRT1c]}{[SIRT1c]+j_{sirt1}}[P53ca] - k_{dp53}([MDM2cp] + [MDM2c])\frac{[P53c]}{[P53c]+j_{1p53}} - k_{dp530}[P53c] - k_i([P53c] - [P53n]) - k_{asp2}[P53c][BCL-2] + k_{dsp2}[P53c \bullet BCL-2], \tag{5}$$

$$\frac{d[P53ca]}{dt} = k_{acp530}[P53c] - k_{dep53}\frac{[SIRT1c]}{[SIRT1c]+j_{sirt1}}[P53ca] - k_{dp53s}([MDM2cp] + [MDM2c])\frac{[P53ca]}{[P53ca]+j_{1p53}} - k_i[P53ca]. \tag{6}$$

Referring to the equations for P53 and SIRT1, the equations of MDM2 are easy to understand. In particular, the P53-dependent synthesis of MDM2 is expressed as a Hill function [15,16], such as the second term of Eq. 7. The Hill coefficient is 4 because P53 binds DNA in a tetrameric form [54]. Although the phosphorylation/dephosphorylation of MDM2 in Fig. 2 is spontaneous, there are actually enzymes involved [51]. These enzymes are omitted, but retain the Michaelis–Menten function form, such as the last two terms of Eq. 7. DNA damage will accelerate the degradation rate of MDM2 in the nucleus [50], which is reflected in the first term of Eq. 9.

$$\frac{d[MDM2c]}{dt} = k_{smdm20} + k_{smdm2}\frac{[P53na]^4}{[P53na]^4 + j_{smdm2}^4} - k_{mdm20}[MDM2c] + k_{1mdm2s}\frac{[MDM2cp]}{[MDM2cp]+j_{1mdm2s}} - k_{mdm2s}\frac{[MDM2c]}{[MDM2c]+j_{mdm2s}}, \tag{7}$$

$$\frac{d[MDM2cp]}{dt} = -k_{1mdm2s}\frac{[MDM2cp]}{[MDM2cp]+j_{1mdm2s}} + k_{mdm2s}\frac{[MDM2c]}{[MDM2c]+j_{mdm2s}} - k_{mdm20}[MDM2cp] - k_i([MDM2cp] - [MDM2np]), \tag{8}$$

$$\frac{d[MDM2np]}{dt} = -(k_{mdm20} + k_{mdm21}\frac{[Dam]}{[Dam]+j_{dam}})[MDM2np] + V_r k_i([MDM2cp] - [MDM2np]). \tag{9}$$

For the **BCL-2** family module, some differential equations of slow variables can be simplified into algebraic equations via the quasi steady state approximation 12]. Moreover, it is assumed that the total amount of both BAX and BCL-2 remains unchanged [12].

In other words, regardless of the production and degradation of these two proteins: it should be noted that by taking the derivative of time, algebraic equations also have differential expressions. For example, the derivative of both sides of Eq. 11 is that $\frac{d[BH3\bullet BCL-2]}{dt} = \frac{d[BH3total]}{dt} - \frac{d[BH3]}{dt}$, and the expressions of $\frac{d[BH3]}{dt}$ and $\frac{d[BH3total]}{dt}$ are shown in Eqs. 14 and 15, respectively. Obviously, after binding to BCL-2, the conversion of BAXm to free BAX and the degradation of BH3 are not affected in their model [12]. For simplicity, we assume that the biochemical reactions of degradation and activation of P53c after forming $P53c \bullet BCL-2$ do not occur, as in Eq. 13. Another difference from the P53-MDM2 module is that the process of BAX being activated by BH3 is written as a linear function instead of a Michaelis–Menten function, as the first term of Eq. 17. In fact, the Michaelis–Menten function is approximately linear when the independent variable is not very large.

$$[BCL-2] = [BCL-2total] - [BH3 \bullet BCL-2] - [BAXm \bullet BCL-2] - [P53c \bullet BCL-2], \quad (10)$$

$$[BH3 \bullet BCL-2] = [BH3total] - [BH3], \quad (11)$$

$$[BAXm \bullet BCL-2] = [BAXmtotal] - [BAXm], \quad (12)$$

$$\frac{d[P53c \bullet BCL-2]}{dt} = k_{asp2}[P53c][BCL-2] - k_{dsp2}[P53c \bullet BCL-2], \quad (13)$$

$$\frac{d[BH3]}{dt} = k_{sbh30} + k_{sbh31}\frac{[P53na]^4}{[P53na]^4 + j_{sbh3}^4} - k_{as32}[BH3][BCL-2] + k_{ds32}[BH3 \bullet BCL-2] - k_{dbh3}[BH3], \quad (14)$$

$$\frac{d[BH3toal]}{dt} = k_{sbh30} + k_{sbh31}\frac{[P53na]^4}{[P53na]^4 + j_{sbh3}^4} - k_{dbh3}[BH3total], \quad (15)$$

$$[BAX] = [BAXtotal] - [BAXmtotal], \quad (16)$$

$$\frac{d[BAXm]}{dt} = (k_{f1} + k_{f2}[BH3])[BAX] - k_{asx2}[BAXm][BCL-2] + k_{dsx2}[BAXm \bullet BCL-2] - k_b[BAXm], \quad (17)$$

$$\frac{d[BAXmtoal]}{dt} = (k_{f1} + k_{f2}[BH3])[BAX] - k_b[BAXmtotal]. \quad (18)$$

Unless otherwise stated, the default parameters for simulation are shown in Table 2. These parameter values are mainly derived from the published models, and a small number of parameter values are estimated to produce reasonable dynamic behavior. Due to the scarcity of quantitative data, it is acceptable to use the hypothetical parameter values to qualitatively explore the dynamics of gene networks, as in [16]. For the sake of simplification, the time unit and concentration unit are not introduced.

Because we think that [BAXmtotal] reaching a high steady state is an indicator of apoptosis, the initial conditions in Table 3 select the steady-state set of each protein concentration corresponding to the low steady state of [BAXmtotal] when [Dam] = 0 to depict the unstressed condition.

2.3. Methods

All numerical simulations and bifurcation analysis are completed with free software: XPPAUT (http://www.math.pitt.edu/bard/xpp/xpp.html) and OSCILL8 (http://oscill8.sourceforge.net/). See the website above for the installation and usage of these software. Notably, the method for numerical simulation in XPPAUT environment uses the stiff. In the attachment, we provide an ODE file that can be directly run with the above two software programs.

Table 2
Standard parameters used for simulations.

Parameter	Description	Value	Reference
k_{ssirt}	SIRT1 basal generation rate	0.01	–
k_{dsirt}	SIRT1 basal degradation rate	0.1	–
V_r	Cytoplasm to nucleus volume ratio	10	[32]
k_i	Protein penetration rate of the nuclear membrane	0.06	–
k_{acp530}	P53 basal activation rate	0.02	–
k_{acp531}	DNA damage-induced the maximum P53 activation rate	0.2	[16]
k_{mdm20}	MDM2 basal degradation rate	0.003	[16]
k_{mdm21}	DNA damage-induced the maximum MDM2 degradation rate	0.05	[16]
j_{dam}	Michaelis constant of DNA damage as a kinase	1	[16]
k_{dep53}	SIRT1-induced the maximum P53 deactivation rate	0.4	–
j_{sirt1}	Michaelis constant of SIRT1 as a kinase	0.1	–
k_{dp53s}	MDM2-induced the maximum active P53 degradation rate	0.01	[16]
j_{1p53}	Michaelis constant of MDM2 as a kinase	0.1	[16]
k_{dp53}	MDM2-induced the maximum inactive P53 degradation rate	0.7	[16]
k_{dp530}	P53 basal degradation rate	0.05	[16]
k_{sp53}	P53 basal generation rate	0.2	[16]
k_{smdm20}	MDM2 basal generation rate	0.002	[16]
k_{smdm2}	P53-dependent MDM2 generation rate	0.024	[16]
j_{smdm2}	Michaelis constant of P53-dependent MDM2 production	1	[16]
k_{1mdm2s}	Dephosphorylation rate of cytoplasmic MDM2	0.3	[16]
j_{1mdm2s}	Michaelis constant of MDM2 dephosphorylation	0.1	[16]
k_{mdm2s}	Phosphorylation rate of cytoplasmic MDM2	8	[16]
j_{mdm2s}	Michaelis constant of MDM2 phosphorylation	0.3	[16]
k_{asp2}	Combination rate of P53 andBCL-2	0.8	–
k_{dsp2}	Dissociation rate of P53 andBCL-2 complex	0.1	–
k_{f1}	Basal rate of BAX to BAXm conversion	1	[12]
k_{f2}	BH3-induced rate of BAX to BAXm conversion	3	[12]
k_{asx2}	Combination rate of BAXm andBCL-2	90	[12]
k_{dsx2}	Dissociation rate of BAXm andBCL-2 complex	0.05	[12]
k_b	Basal rate of BAXm to BAX conversion	2	[12]
k_{sbh30}	BH3 basal generation rate	0.1	–
k_{sbh31}	P53-dependent BH3 generation rate	0.306	–
j_{sbh3}	Michaelis constant of P53-dependent B3 production	0.01	–
k_{as32}	Combination rate of BH3 andBCL-2	90	[12]
k_{ds32}	Dissociation rate of BH3 andBCL-2 complex	0.01	[12]
k_{dbh3}	BH3 basal degradation rate	0.01	[12]
[BAXtotal]	Total level of BAX	100	[12]
[BCL – 2total]	Total level ofBCL-2	80	[12]

3. Results

In this section, we carry out numerical experiments *in silico* to determine the dynamic features of this protein system upon DNA damage. The DNA damage level [Dam] and SIRT1 production parameter k_{ssirt} are the focus of attention so that we can achieve our research purpose.

Table 3
Initial value used in simulations.

Protein	Initial	Protein	Initial	Protein	Initial	Protein	Initial
[P53na]	0.015	[P53n]	0.01	[P53ca]	0.005	[P53c]	0.08
[MDM2c]	0.01	[MDM2cp]	0.6	[MDM2np]	0.59	[SIRT1c]	0.09
[SIRT1n]	0.08	[P53 • BCL − 2]	4.2	[BAXm]	0.12	[BH3]	0.01
[BAXmtotal]	34.06	[BH3total]	35.44				

3.1. Time series analysis

In the slight DNA damage scenario in Fig. 3A, the concentration of P53 slowly increases and reaches a new equilibrium. Obviously, under the stimulation of DNA damage, the content of P53 is higher than that in the background level not only in the nucleus but also in the cytoplasm. A similar phenomenon has been reported in the U-2 OS cell line treated with etoposide [55]. Moreover, there is mostly inactive P53 in the nucleus, which means that the P53 transcription-dependent apoptotic pathway is not activated. Therefore, the total amount of BAXm increases slightly without full activation. That is, cells survive with low DNA damage. Importantly, this mechanism is needed for cells to adapt to internal DNA damage, such as DNA damage during division.

In the moderate DNA damage scenario in Fig. 3B, active P53 predominates in the nucleus; thus, the direct and indirect pathways by which P53 promotes apoptosis are unblocked. Eventually, cell death occurs when BAX is fully activated. Because this model does not reflect what happens after apoptosis, the time series that occurs after BAXm reaches a high steady state is invalid. Hence, P53 will have two phases of dynamics before apoptosis. In the first phase, P53 increases slowly and monotonically, and in the second phase, P53 bursts. It should be noted that the decrease in P53 after the burst may not exist because apoptosis has already been initiated. Indeed, apoptotic cells accompanied by a sudden burst increase in the concentration of P53 have been experimentally found in the MCF7 cell line treated with doxorubicin [56], which is in line with our model. Furthermore, the two-phase dynamics pattern of P53 has also been widely mentioned in theoretical and experimental studies [15,16,56,57]. In our model, the appearance of the second-phase P53 dynamics depends on the interplay between the P53 module and the BAX switch. That is, a large number of substitution reactions occurred at the instant of the burst increase of BAXm, causing P53c• BCL-2 to become BAXm• BCL-2 and P53c monomers. Thereby, we assert that the burst of the P53 concentration first appears in the cytoplasm and will pass to the nucleus after a time delay before apoptosis. This is worthy of further experimental testing.

In the severe DNA damage scenario in Fig. 3C, the dynamics of each node in the network are qualitatively similar to Fig. 3B. The significant difference is that the apoptosis time is advanced in response to severe DNA damage. Taking into account the heterogeneity of individual cells, the time for BAX complete activation in the population of cells is not uniform. Accordingly, our model indicates that as genotoxic pressure increases, the percentage of apoptotic cells observed within a certain period of time will be increased, which has been proven by the experiments in [58]. To further illustrate the relationship between apoptosis time and the degree of DNA damage, we drew Fig. 4A. Regardless of the rate of SIRT1 generation, [Dam] is negatively correlated with apoptosis time. More specifically, as [Dam] increases, the apoptosis time becomes increasingly shorter and eventually approaches a specific shortest time. In contrast, as [Dam] decreases, the apoptosis time will increase unrestricted until it reaches infinity. Biologically, the occurrence of apoptosis at infinite time is equivalent to the fact that apoptosis will never occur.

In Fig. 4A, an interesting phenomenon is that the red and blue lines are both above the black line, which means that apoptosis time will be delayed if the SIRT1 content is too high (Fig. 4A blue line) or too low (Fig. 4A red line). Therefore, we predict that in future experiments, a decrease as well as an increase in SIRT1 levels will both possibly trigger a high rate of apoptosis in the population of cells, depending on the basal SIRT1 expression level. In general, enhanced apoptotic ability can be indicative of antitumor activity [14]. Therefore, our model qualitatively explains the two sides of SIRT1 in cancer development. In the case of SIRT1 overdose, reducing SIRT1 is beneficial to apoptosis and antitumor activity, reflecting the dark side of SIRT1 [48]. In the case of SIRT1 underdose, increasing SIRT1 is conducive to apoptosis and antitumor activity, reflecting the bright side of SIRT1 [49]. A more intuitive display of these viewpoints is shown in Fig. 4B. Regardless of moderate or severe DNA damage (Fig. 4B black or blue line, respectively), the function curve of apoptosis time versus SIRT1 generation rate is U-shaped. This shows that the content of SIRT1 has an optimal value, at which the aim of preventing tumors is the best. In our model, the best SIRT1 production rate was in the interval [0.001, 0.1] in Fig. 4B. Intriguingly, this best value range of k_{ssirt} can also be found by bifurcation analysis; see the subsections below for details.

3.2. One-dimensional bifurcation analysis

Bifurcation is essential to study the dynamic behavior of bistable switches. In particular, the most common switching behavior is the result of the folding of a one-dimensional bifurcation curve, which is Z-shaped or S-shaped. The folding position of the curve is called the saddle node bifurcation point (SN). Thereby, SN plays an important role in the BAX switch. In addition, another type of bifurcation, the Hopf bifurcation point (HB), is ubiquitous in the P53 module. HB is the critical point for the system to transition from steady state to oscillation. As mentioned in the introduction, the model that distinguishes nucleocytoplasmic localization can bring a delay for the P53-MDM2 NFL [33], giving the system the potential to oscillate. Our model therefore contains the two major oscillation elements, i.e., NFL and time delay, and it is anticipated that HB can appear. More specifically, HB includes supercritical (sup-HB) and subcritical (sub-HB). The oscillations born from sup-HB are stable, while the oscillations born from sub-HB are unstable.

Because DNA damage is the input signal, we first use [Dam] as the bifurcation parameter. Fig. 5A shows an S-shaped bifurcation curve. There are only two stable steady states of [BAXmtotal], high or low. The steady state in the middle is unstable. There are also unstable limit cycle oscillations near sub-HB. Such oscillations will occur under only the ideal conditions. Due to the presence of noise in biochemical reactions and inaccuracy in numerical integration, these oscillations will not appear in either biological experiments or computer simulations. Similarly, unstable steady state will not appear in practice. Clearly, the [Dam] threshold required to turn on the BAX switch is reduced from SN2 to sub-HB, which is different from [12]. When the SIRT1 generation rate is extremely small, Fig. 5B shows that SN disappears and the bifurcation curve

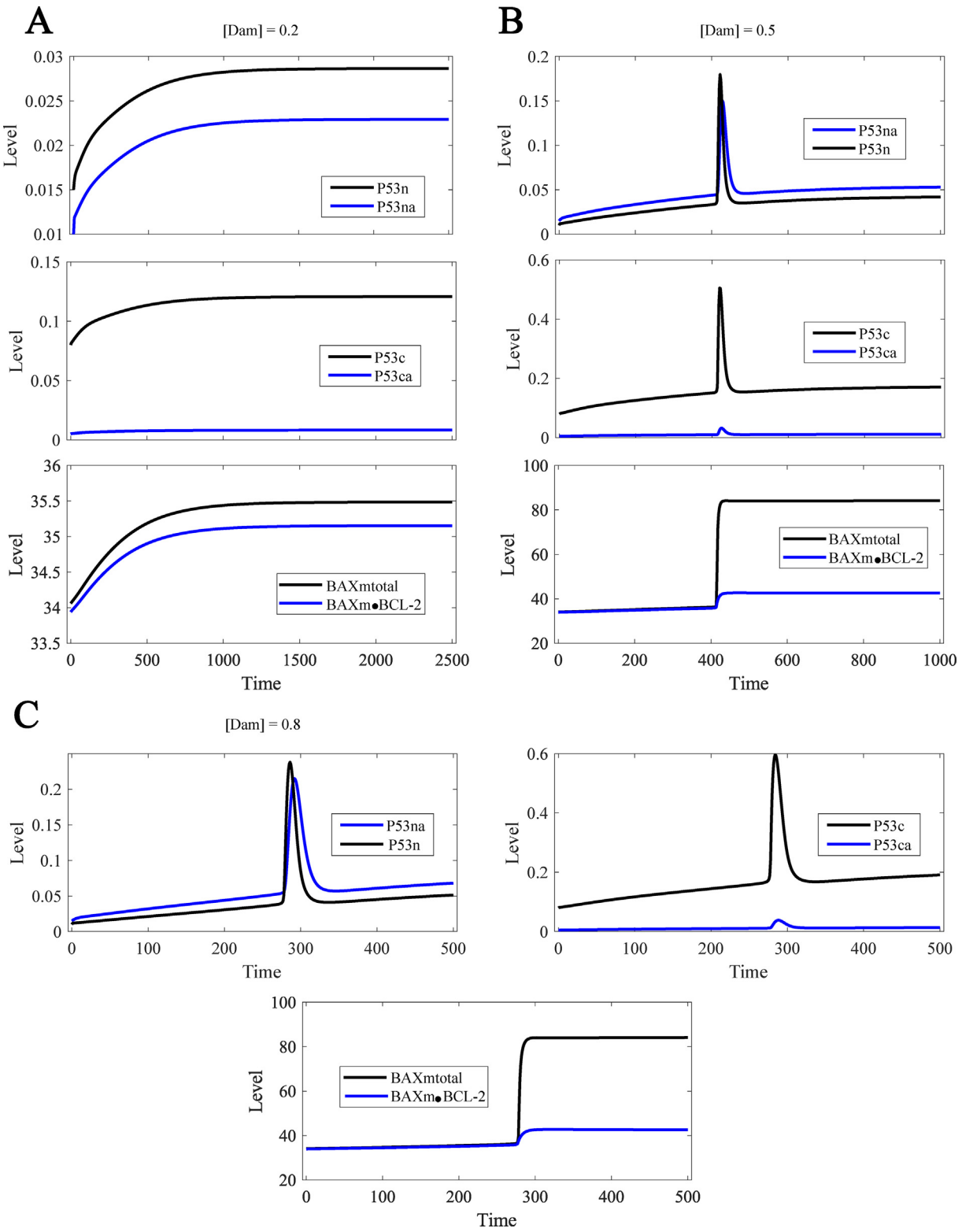

Fig. 3. Time occurs of [P53n], [P53na], [P53c], [P53ca], [BAXmtotal], and [BAXm • BCL − 2] under distinct DNA damage levels: [Dam] = 0.2 **(A)**, 0.5 **(B)**, or 0.8 **(C)**. Increased damage will shorten the time of apoptosis and apoptosis causes all forms of P53 to appear with two-stage kinetics before the BAX switch is turned on.

becomes two parallel horizontal lines. Compared with Fig. 5A, the [Dam] threshold in Fig. 5B is increased (sub-HB moves to the right direction), indicating that only greater DNA damage level can induce apoptosis when SIRT1 is scarce. In the above two cases of Figs. 5A and 5B, the BAX switch is irreversible, i.e., once [BAXmtotal] reaches a highly stable steady state driven by DNA damage, it will maintain the high steady state even if the input signal of DNA damage is removed (i.e., [Dam] = 0). However, in the case of SIRT1 overdose in Fig. 5C, the BAX switch becomes reversible. That is, a strong input signal will turn on the switch, and a weak input signal will turn off the switch. Such a switch is unreliable for cell fate decision-making because the cell may abolish the previous apopto-

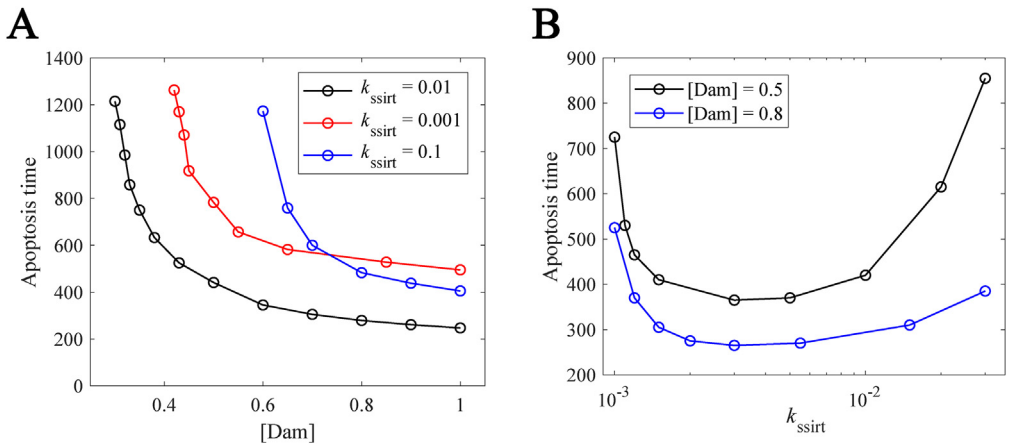

Fig. 4. Apoptosis time as a function of [Dam] **(A)**, or k_{ssirt} **(B)** in different situations. DNA damage always favors apoptosis, while SIRT1 is sometimes beneficial and sometimes not beneficial to apoptosis.

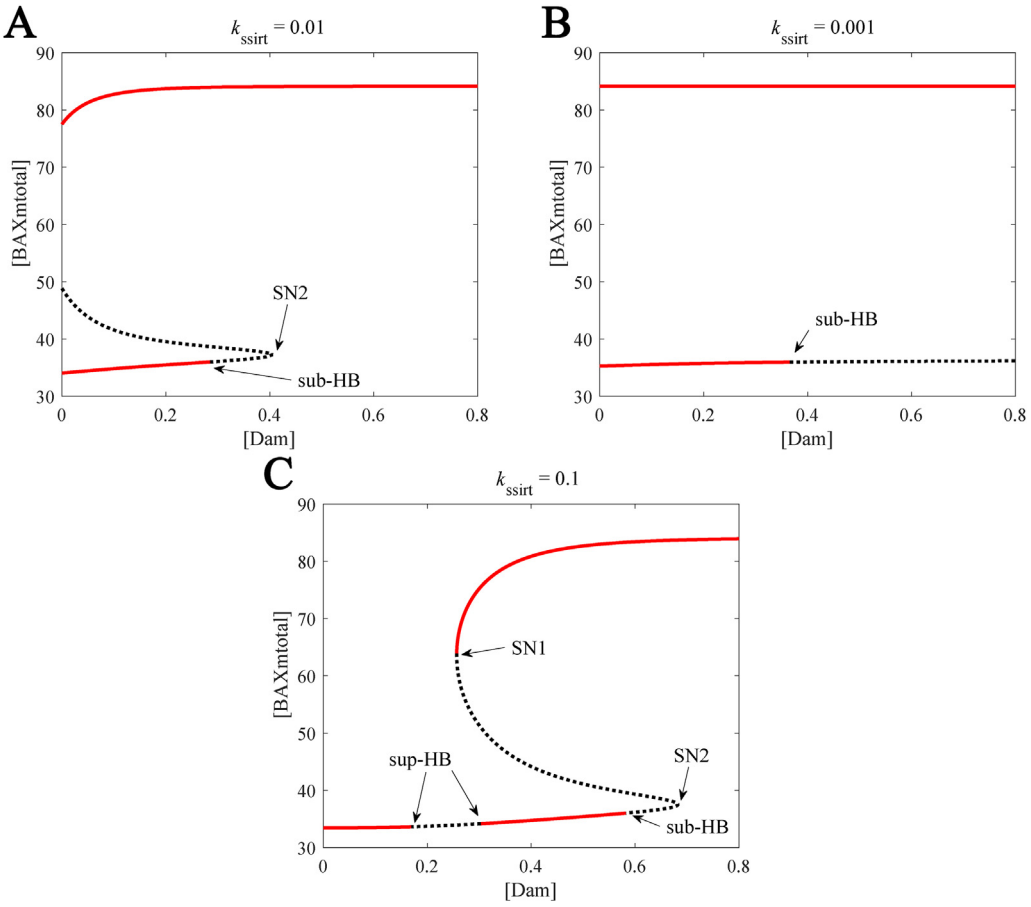

Fig. 5. The relationship between the equilibrium state of active BAX and the degree of DNA damage. Bifurcation diagram of [BAXmtotal] as a function of [Dam] in the case of k_{ssirt} = 0.01 **(A)**, 0.02 **(B)**, or 0.03 **(C)**. The stable and unstable steady states are indicated by red solid and black dotted lines, respectively (the same below). Overexpressed or underexpressed SIRT1 will increase the threshold for BAX switch opening. The overexpression of SIRT1 makes the BAX switch reversible.

sis decision and may violate the checkpoint mechanism. In addition, the sub-HB in Fig. 5C is also to the right of the sub-HB in Fig. 5A. Therefore, even if apoptosis can occur when SIRT1 is overexpressed, a large degree of DNA damage is required. In a word, SIRT1 levels that are too high or too low will raise the threshold of the BAX switch, thereby inhibiting apoptosis.

Interestingly, the lower branch of the S-shaped bifurcation curve in Fig. 5C has a pair of sup-HB, and between them, the stable low steady state of [BAXmtotal] is replaced by a stable oscillation. We show the corresponding time series in Fig. 6. The total concentration of BAXm fluctuates around the basal level, and the cells do not undergo apoptosis. Correspondingly, oscillations also occur in various forms of P53. In biological experiments, P53 oscillations tend to induce cell cycle arrest rather than apoptosis [24,55,58]. Otherwise, long-lasting oscillations of P53 will not be frequently found. Based on these facts, we regard P53 oscillation as an indica-

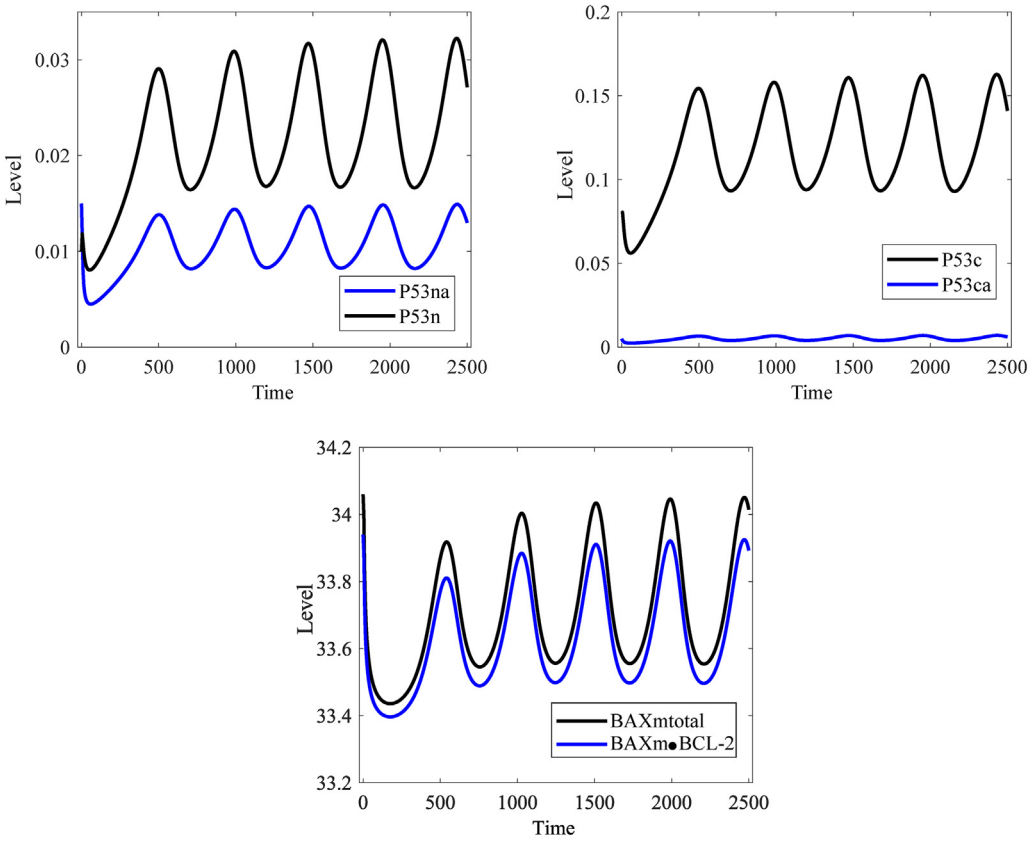

Fig. 6. Time occurs of [P53n], [P53na], [P53c], [P53ca], [BAXmtotal], and [BAXm • BCL − 2] in the case of [Dam] = 0.2 and k_{ssirt} = 0.1. P53 oscillation fails to turn on the BAX switch, but the cell cycle is arrested.

tor of cell cycle arrest, although cells with P53 oscillation dynamics sometimes die a long time afterward [56]. Therefore, high levels of SIRT1 may cause cell cycle arrest. More interestingly, SIRT1 overexpression was found to inhibit cell proliferation in the MCF-7 cell line [59], which is in good agreement with this model. In summary, when SIRT1 is overexpressed, lower DNA damage drives P53 periodic pulsing-regulated cell cycle arrest, and higher DNA damage drives P53 monotonic increase and apoptosis. These results fit the bimodal switch of P53 dynamics and cell outcomes in [55,58] well. We therefore predict that a high content of SIRT1 is beneficial to the emergence of P53 bimodal kinetics, which needs to be verified by biological experiments in the future.

Next, we used the generation rate of SIRT1 as the bifurcation parameter. In the case of mild DNA damage in Fig. 7A, the bifurcation curve is Z-shaped. In the parameter area before SN1, the BAX switch can be opened or closed, depending on the historical state of the system. Accordingly, both cell survival and death are possible. The BAX switch is turned off in the parameter area after SN1, indicating the cancer-promoting effect of SIRT1. In the parameter area after sup-HB, P53 oscillates and induces cell cycle arrest. It is verified again that high levels of SIRT1 are necessary for P53 oscillation and cell cycle arrest. In the case of moderate DNA damage in Fig. 7B, the bifurcation curve is Ω-shaped and spliced by S-shapes and Z-shapes. The high steady state of [BAXmtotal] is always stable, while the stable low steady state only exists in the area outside the two sub-HBs. In other words, higher or lower SIRT1 levels give cells a chance to survive; thus, the dual role and optimal mechanism of SIRT1 levels in mitochondrial apoptosis are vividly demonstrated. In the case of severe DNA damage in Fig. 7C, the bifurcation curve is S-shaped. When the rate of SIRT1 production exceeds sub-HB, apoptosis will inevitably occur, and the cancer-inhibiting effect of SIRT1 is presented.

Of note, from the perspective of a stable steady state distribution, the bifurcation diagram in Fig. 7C shows that the larger k_{ssirt} is, the more advantageous the BAX switch is turned on when [Dam] = 0.8. However, the blue line in Fig. 4B shows that the dual role of SIRT1 still exists from the perspective of apoptosis time. Therefore, we believe that the dual function of SIRT1 in tumor formation is robust and insensitive to the degree of DNA damage.

3.3. Two-dimensional bifurcation analysis

Finally, we make a codimension two bifurcation diagram to more comprehensively exhibit the stable dynamics distribution of the system in the ([Dam], k_{ssirt}) parameter plane. Fig. 8 is easily obtained by extending the bifurcation points in Fig. 5C. However, if the unstable limit cycle is taken into account, the codimensional two bifurcation graph will be more complicated, and other types of bifurcation points need to be extended, such as the homoclinic bifurcation point. Due to the specificity of the goal of our research, these complex bifurcations are not considered.

The ([Dam], k_{ssirt}) parameter plane is divided into six areas by these bifurcation lines:

- R_1: [BAXmtotal] is in low steady state, cell survival;
- R_2: [BAXmtotal] oscillates near the low steady state, cell cycle arrest;
- R_3: [BAXmtotal] is in high steady state or oscillates near the low steady state, cell death or cell cycle arrest;
- R_4: [BAXmtotal] is in low or high steady state, cell survival or death;
- R_5: [BAXmtotal] is in high steady state, cell death;
- R_6: [BAXmtotal] is in high steady state, cell death.

The R_5 region and the R_6 region have the same recurrent dynamics, but their transient dynamics are different. Strictly

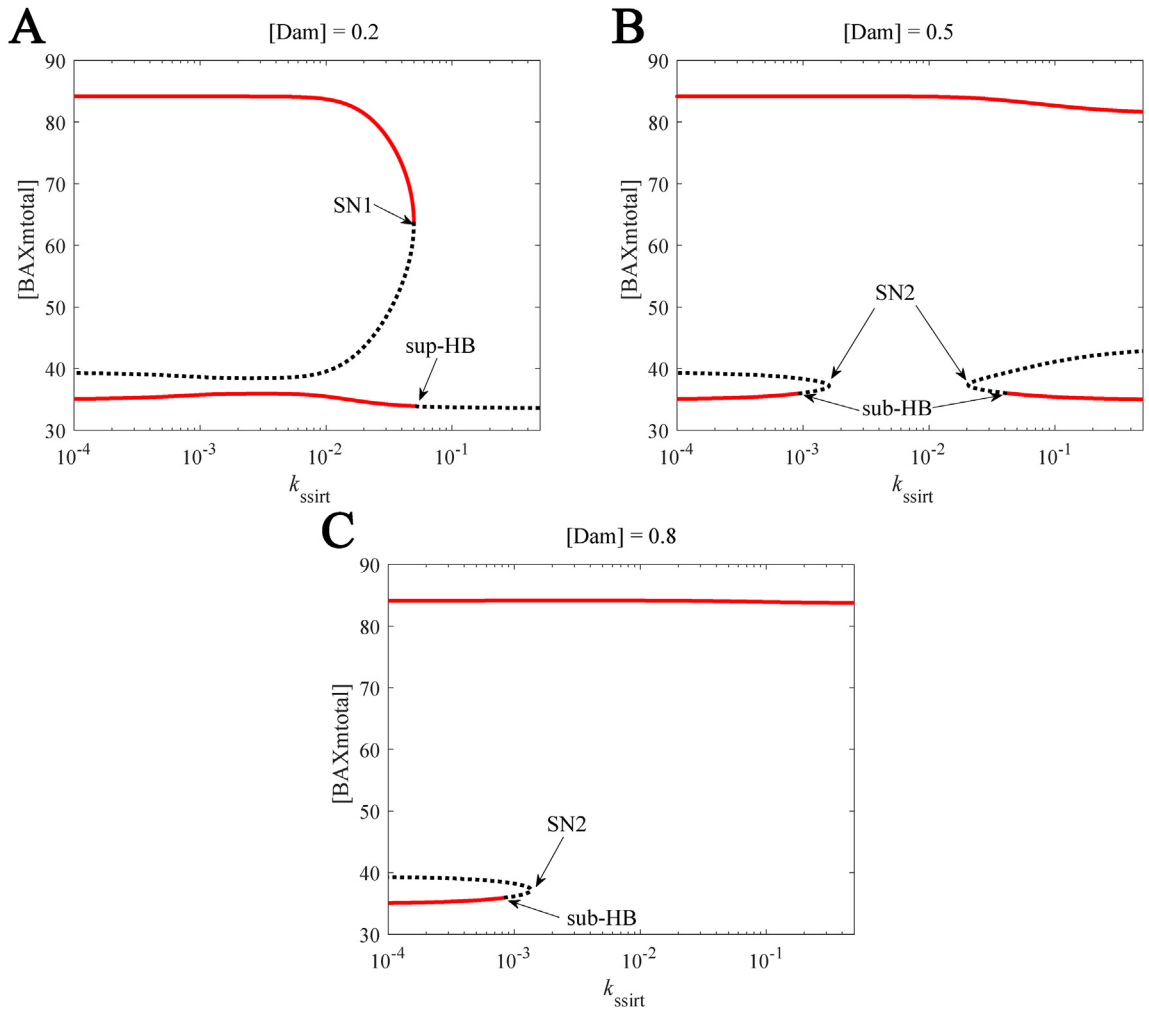

Fig. 7. The relationship between the equilibrium state of active BAX and SIRT1 production rate. Bifurcation diagram of [BAXmtotal] as a function of k_{ssirt} in the case of [Dam] = 0.2 **(A)**, 0.5 **(B)**, or 0.8 **(C)**. Excessive SIRT1 will destroy the high steady state of active BAX at the low level of DNA damage. Moderate SIRT1 will force active BAX to reach a high steady state at the moderate level of DNA damage. Too little SIRT1 will allow active BAX to reside in a low steady state at a high level of DNA damage.

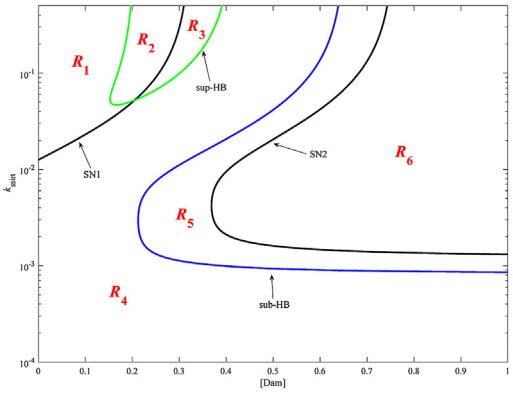

Fig. 8. Codimension two bifurcation diagram showing various types of bifurcation lines in the (DNA damage level, SIRT1 synthesis rate)-plane. The black line is the SN line, the green line is the sup-HB line, and the blue line is the sub-HB line. These bifurcation lines divide the parameter domain into six subdomains $R_1 \ldots, R_6$. The steady states and cellular outcomes in each of these domains are given in main text.

speaking, the R_5 region is an excitable parameter region (i.e., one stable steady state coexist with two unstable steady states), where the trajectory of the dynamic system is very different. To our knowledge, excitability may actually exist in the E2F protein network [60], P53 protein network [61], and so on. However, the excitability of the BAX protein network in our model is experimentally unobservable. The excitability in this model means that when [BAXmtotal] is in a high steady state, if and only if the cell does not undergo apoptosis, a disturbance will cause [BAXmtotal] to return to the basal level briefly.

In addition, the sub-HB line and SN2 line in Fig. 8 clearly show again that the optimal value range of the SIRT1 generation rate for cell apoptosis is [0.001, 0.01], in which the BAX switch is most sensitive to the input signal of DNA damage. This parameter interval is in good agreement with Fig. 4B. Moreover, if k_{ssirt} is lower than the optimal value range, the direct pathway of P53 to promote apoptosis is blocked. Although apoptosis is possible in this condition, it cannot be triggered by DNA damage. Alternatively, if k_{ssirt} is greater than the optimal value range, the BAX switch is changed from one-way to be toggled due to the appearance of the SN1 line, and apoptosis needs DNA damage to be maintained at a sufficiently high level in this case. Fig. 8 also indicates that repeated pulses of P53 may be a sign of SIRT1 overdose, and then the levels of SIRT1 need to be lowered to restore the sensitivity of tumor cells to genotoxic drugs. However, when the cells are extremely resistant to genotoxic drugs, the reason may be that SIRT1 is underdosed, and then the effectiveness of SIRT1 needs to be strengthened to achieve anticancer effects. All in all, if SIRT1 is used as an anticancer target in

clinical practice, attention should be given to the dual role and optimal concentrations mechanism of SIRT1.

4. Discussion

Traditionally, the **BCL-2** family is divided into three subcategories [8]. Among them, the BAX-like protein is the executor of apoptosis, and its conformation and cell sublocalization are changed under stress [6]. Behind the biochemical reactions of **BCL-2** family proteins, there is a potential switch dynamic behavior responsible for apoptosis [4,11,12]. P53 is a common upstream protein of the **BCL-2** family, which directly or indirectly participates in the biochemical reactions of the **BCL-2** family. Essentially, SIRT1 maintains the balance between the direct and indirect participation of P53 in biochemical reactions with the **BCL-2** family [44], thereby making the apoptosis mechanism more reliable. The subject of our research is a mathematical model of the crosstalk between P53 and **BCL-2** family, and the connection between SIRT1 and apoptosis is the focus of attention.

SIRT1 is well known for binding and deacetylating the C-terminal Lys382 residue of P53. Vaziri et al. revealed that not only is the transcriptional activity of P53 is suppressed by SIRT1 but also P53-dependent apoptosis and radiosensitivity are potentiated in human cells when SIRT1 activity is repressed [45]. However, Han et al. reported that SIRT1 increases the sensitivity of mouse cells to reactive oxygen species by blocking P53 nuclear translocation and triggering mitochondrial-dependent apoptosis [46]. In our mathematical model, these seemingly contradictory phenomena are reconciled. The model showed that SIRT1 has the optimal content for killing cancer cells by flipping the BAX switch. Furthermore, SIRT1 is higher than, rather than lower than or equal to its optimal content, which may support the oscillation of the P53 module in the model.

In fact, the addition of SIRT1 to the P53-mediated cell fate decision network model has been investigated in the past few years [62]. Findings have emphasized the dark side of SIRT1, that is, inhibiting apoptosis and promoting cancer. In this way, the tumor suppressor function of miR-34 was demonstrated, consistent with experimental observations [63]. In the current work, we highlight the dual role of SIRT1; on the one hand, promoting the direct apoptosis pathway of P53, and on the other hand, inhibiting the indirect apoptosis pathway of P53 [44]. If the miR-34-mediated inhibition of SIRT1 is considered in our model, the scenario in which miR-34 inhibits apoptosis is still appropriate, but this is not always the case: miR-34 will hinder apoptosis and facilitate cancer when k_{ssirt} is lower than the optimal value. Even, miR-34 may display more anticancer properties in biomedicine practice. Concretely, miR-34 has various tumor suppressor pathways. As mentioned above, miR-34 blocks the translation ofBCL-2 [39]. In addition, miR-34 affects the enzymatic activity of MDM2 by blocking the expression of MDM4 [64]. These anticancer pathways provide multiple options for miR-34 to suppress cancer.

Of course, the phenotypes and genotypes of cancer cells are diverse, and the applicability of our model is limited, like many other modeling studies. Perhaps this research is more suitable for tumor types where the problem lies in the SIRT1-P53 axis. Due to the intricate biochemical reactions and huge regulatory network, mathematical models are indispensable for understanding system dynamics. However, deeper modeling studies need to clarify cell types and even pressure types [65]. In addition, to avoid complexity, this model does many simplifications. There are many points that can be considered in future protein network modeling studies, such as P53 transactivates BAX and P53 inhibit BCL-2, P53 promotes DNA repair, etc. Furthermore, our model portrays the single-cell level. A more macroscopic model can be established at the population cell level [66], and a more microscopic model can be established at the molecular level [67]. We think it will be important to link these different level models to each other.

5. Conclusions

In this article, we developed a new model based partly on the model published in [12] to characterize the dual role of SIRT1 in apoptosis. We trust the switch mechanism in the cell fate decision and choose the BAX switch as a marker for apoptosis. In our model, the P53 module is used as the sensor before the BAX switch, where SIRT1 directly performs its function. To study the dynamic behavior of a switch, time series analysis and bifurcation analysis are necessary. The time series suggested that the abundance or lack of SIRT1 concentration will delay the activation of the BAX switch and reduce the probability of apoptosis. The dual role and optimal concentration mechanism of SIRT1 emerged. In addition, both the codimensional one-dimensional bifurcation graphes and the '<'-shaped bifurcation lines in the two-dimensional bifurcation analysis verified these viewpoints. We further proposed that the burst of P53 before apoptosis occurs first in the cytoplasm, and a high expression level of SIRT1 is conducive to the bimodal switch of P53 dynamics. These results are of great importance and deserve further research.

Declaration of Competing Interest

The authors declare that they have no known competing financial interests or personal relationships that could have appeared to influence the work reported in this paper.

Acknowledgement

This work was supported by grant from National Natural Science Foundation of China (11762011) and Natural Science Foundation of Inner Mongolia Autonomous Region of China (Grants No. 2021ZD01).

Appendix A. Supplementary data

Supplementary data associated with this article can be found, in the online version, at https://doi.org/10.1016/j.csbj.2021.09.033.

References

[1] Bi Y, Yang Z, Meng X, Lu Q. Noise-induced bistable switching dynamics through a potential energy landscape. Acta Mech Sin 2015;31:216–22.
[2] Yao G, Lee TJ, Mori S, Nevins JR, You L. A bistable Rb-E2F switch underlies the restriction point. Nat Cell Biol 2008;10:477–82.
[3] Wee KB, Aguda BD. Akt versus p53 in a network of oncogenes and tumor suppressor genes regulating cell survival and death. Biophys J 2006;91:857–65.
[4] Chen C, Cui J, Lu H, Wang R, Zhang S, Shen P. Modeling of the Role of a Bax-Activation Switch in the Mitochondrial Apoptosis Decision. Biophys J 2007;92:4304–15.
[5] Kang X, Li C. Landscape inferred from gene expression data governs pluripotency in embryonic stem cells. Comput Struct Biotech 2020;18:366–74.
[6] Schinzel A, Kaufmann T, Borner C. Bcl-2 family members: intracellular targeting, membrane-insertion, and changes in subcellular localization. Biochim Biophys Acta 2004;1644:95–105.
[7] Kalkavan H, Green DR. MOMP, cell suicide as a BCL-2 family business. Cell Death Differ 2018;25:46–55.
[8] Lee EF, Fairlie WD. Structural biology of the intrinsic cell death pathway: what do we know and what is missing? Comput Struct Biotech 2012;1:e20120400.
[9] Teijido O, Dejean L. Upregulation of Bcl2 inhibits apoptosis-driven BAX insertion but favors BAX relocalization in mitochondria. FEBS Lett 2010;584:3305–10.
[10] Walensky LD, Pitter K, Morash J, Oh KJ, Barbuto S, Fisher J, Smith E, Verdine GL, Korsmeyer SJ. A stapled BID BH3 helix directly binds and activates BAX. Mol Cell 2006:24;199–210..
[11] Sun T, Lin X, Wei Y, Xu Y, Shen P. Evaluating bistability of Bax activation switch. FEBS Lett 2010;584:954–60.

[12] Zhang T, Brazhnik P, Tyson JJ. Computational analysis of dynamical responses to the intrinsic pathway of programmed cell death. Biophys J 2009;97:415–34.
[13] Hat B, Kochaczyk M, Bogda MN, Lipniacki T. Feedbacks, bifurcations, and cell fate decision-making in the p53 system. PLoS Comput Biol 2016;12:e1004787.
[14] Cory S, Adams JM. Killing cancer cells by flipping the Bcl-2/Bax switch. Cancer Cell 2005;8:5–6.
[15] Sun CY, Zhang XP, Wang W. Coordination of miR-192 and miR-22 in p53-Mediated Cell Fate Decision. Int J Mol Sci 2019;20:4768.
[16] Zhang XP, Liu F, Wan W. Two-phase dynamics of p53 in the DNA damage response. Proc Natl Acad Sci USA 2011;108:8990–5.
[17] Sun T, Chen F, Wu Y, Zhang S, Cui J, Shen P. Modeling the role of p53 pulses in DNA damage-induced cell death decision. BMC Bioinf 2009;10:190.
[18] Kheraldine H, Gupta I, Alhussain H, Jabeen A, Cyprian FS, Akhtar S, Al Moustafa AE, Rachid O. Substantial cell apoptosis provoked by naked PAMAM dendrimers in HER2-positive human breast cancer via JNK and ERK1/ERK2 signalling pathways. Comput Struct Biotech 2021;19:2881–90.
[19] Yael A, Moshe O. Living with p53, dying of p53. Cell 2007;130:597–600.
[20] Vogelstein B, Lane D, Levine A. Surfing the p53 network. Nature 2000;408:307–10.
[21] Bar-Or RL, Maya R, Segel LA, Alon U, Levine AJ, Oren M. Generation of oscillations by the p53-Mdm2 feedback loop: a theoretical and experimental study. Proc Natl Acad Sci USA 2000;97:11250–5.
[22] Hamstra DA, Bhojani MS, Griffin LB, Laxman B, Ross BD, Rehemtulla A. Real-time evaluation of p53 oscillatory behavior in vivo using bioluminescent imaging. Cancer Res 2006;66:7482–9.
[23] Stewart-Ornstein J, Cheng HWJ, Lahav G. Conservation and divergence of p53 oscillation dynamics across species. Cell Syst 2017;5:e414.
[24] Purvis JE, Karhohs KW, Caroline M, Eric B, Alexander L, Galit L. p53 dynamics control cell fate. Science 2012;336:1440–4.
[25] Gao C, Liu H, Yan F. Dynamic behavior of p53 driven by delay and a microrna-34a-mediated feedback loop. Int J Mol Sci 2020;21:1271.
[26] Bi Y, Yang Z, Zhuge C, Lei J. Bifurcation analysis and potential landscapes of the p53-Mdm2 module regulated by the co-activator programmed cell death 5. Chaos 2015;25:821–9.
[27] Wang C, Yan F, Liu H. Theoretical study on the oscillation mechanism of p53-Mdm2 network. Int J Biomathe 2018;11:1850112.
[28] Liu N, Yang H, Yang L. Exploring the influence of microRNA miR-34 on p53 dynamics: a numerical study. Commun Theor Phys 2021;73:035601.
[29] Liu N, Yang H, Li S, Wang D, Yang L. Oscillation and bistable switching dynamical behavior of p53 regulated by PTEN upon DNA damage. Acta Mech Sin 2021;37:712–23.
[30] Gao C, Chen F. Oscillatory Behaviors of Delayed p53 Regulatory Network with microRNA 192 in DNA Damage Response. Int J Bifur Chaos 2021;31:2150020.
[31] Haupt Y, Maya R, Kazaz A, Oren M. Mdm2 promotes the rapid degradation of p53. Nature 1997;387:296–9.
[32] Elias J, Dimitrio L, Clairambault J, Natalini R. The dynamics of p53 in single cells: Physiologically based ODE and reaction-diffusion PDE models. Phys Biol 2014;11:045001.
[33] Puszynski K, Hat B, Lipniacki T. Oscillations and bistability in the stochastic model of p53 regulation. J Theo Biol 2008;254:452–65.
[34] Wang LS, Li NX, Chen JJ, Zhang XP, Liu F, Wang W. Modulation of dynamic modes by interplay between positive and negative feedback loops in gene regulatory networks. Phys Rev E 2018;97:042412.
[35] Bla N, Tyson JJ. Design principles of biochemical oscillators. Nat Rev Mol Cell Biol 2008;9:981–91.
[36] Miyashita T, Reed JC. Tumor suppressor p53 is a direct transcriptional activator of the human bax gene. Cell 1995;80:193–299.
[37] Nakano K, Vousden KH. PUMA, a novel proapoptotic gene, is induced by p53. Mol Cell 2001;7:683–94.
[38] Chang TC, Wentzel EA, Kent OA, Ramachandran K, Mullendore M, Lee KH, Feldmann G, Yamakuchi M, Ferlito M, Lowenstein CJ. Transactivation of mir-34a by p53 broadlyinfluences gene expression and promotes apoptosis. Mol Cell 2007;26:745–52.
[39] Hermeking H. The miR-34 family in cancer and apoptosis. Cell Death Differ 2010;17:193–9.
[40] Moll UM, Wolff S, Speidel D, Deppert W. Transcription-independent pro-apoptotic functions of p53. Curr Opin Cell Biol 2005;17:631–6.
[41] Mihara M, Erster S, Zaika A, Petrenko O, Chittenden T, Pancoska P, Moll UM. P53 has a direct apoptogenic role at the mitochondria. Mol Cell 2003;11:577–90.
[42] Pu T, Zhang XP, Liu F, Wang W. Coordination of the Nuclear and Cytoplasmic Activities of p53 in Response to DNA Damage. Biophys J 2010;99:1696–705.
[43] Tian XJ, Liu F, Zhang XP, Li J, Wang W. A two-step mechanism for cell fate decision by coordination of nuclear and mitochondrial p53 activities. PLoS One 2012;7:e38164.
[44] Yi J, Luo J. SIRT1 and p53, effect on cancer, senescence and beyond. Biochim Biophys Acta 2010;1804:1684–9.
[45] Vaziri H, Dessain SK, Ng Eaton E, Imai SI, Frye RA, Pandita TK, Guarente L, Weinberg RA. hSIR2(SIRT1) functions as an NAD-dependent p53 deacetylase. Cell 2001;107:149–59.
[46] Han M, Song E, Guo Y, Ou X, Mantel C, Broxmeyer HE. SIRT1 regulates apoptosis and Nanog expression in mouse embryonic stem cells by controlling p53 subcellular localization. Cell Stem Cell 2008;2:241–51.
[47] Bradbury CA, Khanim FL, Hayden R, Bunce CM, White DA, Drayson MT, Craddock C, Turner BM. Histone deacetylases in acute myeloid leukaemia show a distinctive pattern of expression that changes selectively in response to deacetylase inhibitors. Leukemia 2005;19:1751–9.
[48] Huffman DM, Grizzle WE, Bamman MW, Kim J, Eltoum IA, Elgavish A, Nagy TR. SIRT1 is significantly elevated in mouse and human prostate cancer. Cancer Res 2007;67:6612–8.
[49] Wang RH, Sengupta K, Li C, Kim HS, Cao L, Xiao C, Kim S, Xu X, Zheng Y, Chilton B, et al. Impaired DNA Damage Response, Genome Instability, and Tumorigenesis in SIRT1 Mutant Mice. Cancer Cell 2008;14:312–23.
[50] Stommel JM, Wahl GM. Accelerated mdm2 auto-degradation induced by DNA damage kinases is required for p53 activation. EMBO J 2014;23:1547–56.
[51] Mayo LD, Donne DB. A phosphatidylinositol 3-kinase/Akt pathway promotes translocation of mdm2 from the cytoplasm to the nucleus. Proc Natl Acad Sci USA 2001;98:11598–603.
[52] Ciliberto A, Novak B, Tyson JJ. Steady State and Oscillations in the p53/Mdm2 Network. Cell Cycle 2005;4:488–93.
[53] Chehab NH, Malikzay A, Stavridi ES, Halazonetis TD. Phosphorylation of Ser-20 mediates stabilization of human p53 in response to DNA damage. Proc Natl Acad Sci USA 1999;96:13777–82.
[54] Chene P. The role of tetramerization in p53 function. Oncogene 2001;20:2611–7.
[55] Chen X, Chen J, Gan S, Guan H, Zhou Y, Ouyang Q, Shi J. DNA damage strength modulates a bimodal switch of p53 dynamics for cell-fate control. BMC Biol 2013;11:73.
[56] Wu M, Ye H, Tang Z, Shao C, Lu G, Chen B, Yang Y, Wang G, Hao H. p53 dynamics orchestrates with binding affinity to target genes for cell fate decision. Cell Death Dis 2017;8:e3130.
[57] Tsabar M, Mock CS, Venkatachalam V, Reyes J, Karhohs KW, Oliver TG, Regev A, Jambhekar A, Lahav G. A Switch in p53 Dynamics Marks Cells That Escape from DSB-Induced Cell Cycle Arrest. Cell Rep 2020;32:107995.
[58] Yang R, Huang B, Zhu Y, Li Y, Liu F, Shi J. Cell typeCdependent bimodal p53 activation engenders a dynamic mechanism of chemoresistance. Sci Adv 2018;4:eaat5077.
[59] Yao Y, Liu T, Wang X, Zhang D. The Contrary Effects of Sirt1 on MCF7 Cells Depend on CD36 Expression Level. J Surg Res 2019;238:248–54.
[60] Aguda BD, Kim Y, Piper-Hunter MG, Friedman A, Marsh CB. MicroRNA regulation of a cancer network: Consequences of the feedback loops involving miR-17-92, E2F, and Myc. Proc Natl Acad Sci USA 2008;105:19678–83.
[61] Monke G, Cristiano E, Finzel A, Friedrich D, Herzel H, Falcke M, Loewer A. Excitability in the p53 network mediates robust signaling with tunable activation thresholds in single cells. Sci Rep 2017;7:46571.
[62] Yan F, Liu H, Liu Z. Dynamic analysis of the combinatorial regulation involving transcription factors and microRNAs in cell fate decisions. Biochim Biophys Acta 2013;1884:248–57.
[63] Yamakuchi M, Ferlito M, Lowenstein CJ. miR-34a repression of SIRT1 regulates apoptosis. Proc Natl Acad Sci USA 2008;105:13421–6.
[64] Okada N, Lin CP, Ribeiro MC, Biton A, Lai C, He X, Bu P, Vogel H, Jablons DM, Keller AC, et al. A positive feedback between p53 and miR-34 miRNAs mediates tumor suppression. Genes Dev 2014;28:438–50.
[65] Batchelor E, Loewer A. Recent progress and open challenges in modeling p53 dynamics in single cells. Curr Opin Syst Biol 2017;3:54–9.
[66] Posadas EM, Criley SR, Coffey DS. Chaotic oscillations in cultured cells: rat prostate cancer. Cancer Res 1996;56:3682–8.
[67] Wang Y, Liu F, Li J, Wang W. Reconciling the concurrent fast and slow cycling of proteins on gene promoters. J.R. Soc. Interface 2014;11:20140253.